MOLLIFYING NETWORKS

Caglar Gulcehre[1], **Marcin Moczulski**[2,*], **Francesco Visin**[3,*] **Yoshua Bengio**[1]
[1] University of Montreal, [2] University of Oxford, [3] Politecnico di Milano

ABSTRACT

The optimization of deep neural networks can be more challenging than traditional convex optimization problems due to the highly non-convex nature of the loss function, e.g. it can involve pathological landscapes such as saddle-surfaces that can be difficult to escape from for algorithms based on simple gradient descent. In this paper, we attack the problem of optimization of highly non-convex neural networks by starting with a smoothed – or *mollified* – objective function which becomes more complex as the training proceeds. Our proposition is inspired by the recent studies in continuation methods: similarly to curriculum methods, we begin by learning an easier (possibly convex) objective function and let it evolve during training until it eventually becomes the original, difficult to optimize, objective function. The complexity of the mollified networks is controlled by a single hyperparameter that is annealed during training. We show improvements on various difficult optimization tasks and establish a relationship between recent works on continuation methods for neural networks and mollifiers.

1 INTRODUCTION

In the last years deep neural networks – i.e. convolutional networks (LeCun et al., 1989), LSTMs (Hochreiter & Schmidhuber, 1997a) or GRUs (Cho et al., 2014) – set the state of the art on a range of challenging tasks (Szegedy et al., 2014; Visin et al., 2015; Hinton et al., 2012; Sutskever et al., 2014; Bahdanau et al., 2014; Mnih et al., 2013; Silver et al., 2016). However when trained with variants of SGD (Bottou, 1998) deep networks can be difficult to optimize due to their highly non-linear and non-convex nature (Choromanska et al., 2014; Dauphin et al., 2014).

A number of approaches were proposed to alleviate the difficulty of optimization: addressing the problem of the internal covariate shift with Batch Normalization (Ioffe & Szegedy, 2015), learning with a curriculum (Bengio et al., 2009) and recently training with diffusion (Mobahi, 2016) - a form of continuation method. The impact of noise injection on the behavior of modern deep models has been explored in Neelakantan et al. (2015) and noisy activation functions have been recently shown to improve performance on a wide variety of tasks (Gulcehre et al., 2016).

We connect the ideas of curriculum learning and continuation methods with those arising from models with skip connections and with layers that compute near-identity transformations. Skip connections allow to train very deep residual and highway architectures (He et al., 2015; Srivastava et al., 2015) by skipping layers or block of layers. Similarly, it has been shown that stochastically changing the depth of a network during training (Huang et al., 2016b) does not prevent convergence and allows to generalize better.

We discuss the idea of mollification for neural networks – a form of differentiable smoothing of the loss function connected to noisy activations – which in our case can be interpreted as a form of adaptive noise injection which is controlled by a single hyperparameter. Inspired by Huang et al. (2016b), we use a hyperparameter to stochastically control the depth of our network. This allows us to start the optimization from a *convex objective function* (as long as the optimized criterion is convex, e.g. linear or logistic regression) and to slowly introduce more complexity into the model by annealing the hyperparameter, thus making the network deeper and increasingly non-linear.

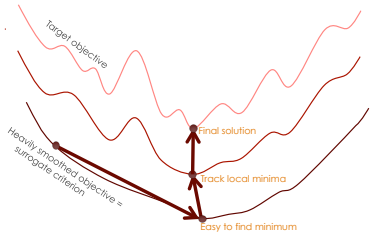

Figure 1: A sequence of optimization problems of increasing complexity, where the first ones are easy to solve but only the last one corresponds to the actual problem of interest. It is possible to tackle the problems in order, starting each time at the solution of the previous one and tracking the local minima along the way.

2 Mollifying Objective Functions

2.1 Continuation and Annealing Methods

Continuation methods and *simulated annealing* provide a general strategy to reduce the impact of local minima and deal with non-convex, continuous, but not necessarily everywhere differentiable objective functions by smoothing the original objective function gradually reducing the amount of smoothing during training (Allgower & Georg, 1980) (see Fig. 1).

In machine learning, approaches based on curriculum learning (Bengio et al., 2009) are inspired by this principle and define a sequence of gradually more difficult training tasks (or training distributions) that eventually converge to the task of interest.

In the context of stochastic gradient descent, we can use an estimator of the gradient of the smoothed objective function. This is convenient because it may not be analytically feasible to compute the smoothed function, but a Monte-Carlo estimate can often be obtained easily.

In this paper we construct a sequence of smoothed objective functions obtained with a form of mollification and we progressively optimize them. The training procedure iterates over the sequence of objective functions starting from the simpler ones – i.e. with a smoother loss surface – and moving towards more complex ones until the last, original, objective function is reached.[1]

2.2 Mollifiers and Weak Gradients

We smooth the loss function $\mathcal{L}$, which is parametrized by $\theta \in \mathbb{R}^n$, by convolving it with another function $K(\cdot)$ with stride $\tau \in \mathbb{R}^n$:

$$\mathcal{L}_K(\boldsymbol{\theta}) = (\mathcal{L} * K)(\boldsymbol{\theta}) = \int_{-\infty}^{+\infty} \mathcal{L}(\boldsymbol{\theta} - \boldsymbol{\tau}) K(\boldsymbol{\tau}) d\boldsymbol{\tau} \tag{1}$$

Although there are many choices for the function $K(\cdot)$, we focus on those that satisfy the definition of a mollifier.

A mollifier is an infinitely differentiable function that behaves like an approximate identity in the group of convolutions of integrable functions. If $K(\cdot)$ is an infinitely differentiable function, that converges to the Dirac delta function when appropriately rescaled and for any integrable function $\mathcal{L}$, then it is a mollifier:

$$\mathcal{L}(\boldsymbol{\theta}) = \lim_{\epsilon \to 0} \int \epsilon^{-n} K(\boldsymbol{\tau}/\epsilon) \mathcal{L}(\boldsymbol{\theta} - \boldsymbol{\tau}) d\boldsymbol{\tau}. \tag{2}$$

If we choose $K(\cdot)$ to be a mollifier and obtain the smoothed loss function $\mathcal{L}_K$ as in Eqn. 1, we can take its gradient with respect to $\boldsymbol{\theta}$ using directly the result from Evans (1998):

$$\nabla_{\boldsymbol{\theta}} \mathcal{L}_K(\boldsymbol{\theta}) = \nabla_{\boldsymbol{\theta}} (\mathcal{L} * K)(\boldsymbol{\theta}) = (\mathcal{L} * \nabla K)(\boldsymbol{\theta}). \tag{3}$$

[*] This work was done while these students were interning at the MILA lab, University of Montreal.

[1] We plan to release the source code of the models and experiments under, `http://github.com/caglar/molly_nets/`.

To relate the resulting gradient $\nabla_{\boldsymbol{\theta}}\mathcal{L}_K$ to the gradient of the original function $\mathcal{L}$, we introduce the notion of weak gradient, i.e. an extension to the idea of weak/distributional derivatives to functions with multidimensional arguments, such as loss functions of neural networks.

For an integrable function $\mathcal{L}$ in space $\mathcal{L} \in L([a,b])$, $\mathrm{g} \in L([a,b]^n)$ is a $n\text{-}dimensional$ weak gradient of $\mathcal{L}$ if it satisfies:

$$\int_C \mathrm{g}(\boldsymbol{\tau})K(\boldsymbol{\tau})d\boldsymbol{\tau} = -\int_C \mathcal{L}(\boldsymbol{\tau})\nabla K(\boldsymbol{\tau})d\boldsymbol{\tau}, \tag{4}$$

where $K(\boldsymbol{\tau})$ is an infinitely differentiable function vanishing at infinity, $C \in [a,b]^n$ and $\boldsymbol{\tau} \in \mathbb{R}^n$.

As long as the chosen $K(\cdot)$ fulfills the definition of a mollifier we can use Eqn. 3 and Eqn. 4 [2] to rewrite the gradient as:

$$\begin{aligned}
\nabla_{\boldsymbol{\theta}}\mathcal{L}_K(\boldsymbol{\theta}) &= (\mathcal{L} * \nabla K)(\boldsymbol{\theta}) && \text{by Eqn. 3} && (5)\\
&= \int_C \mathcal{L}(\boldsymbol{\theta}-\boldsymbol{\tau})\nabla K(\boldsymbol{\tau})d\boldsymbol{\tau} && && (6)\\
&= -\int_C \mathrm{g}(\boldsymbol{\theta}-\boldsymbol{\tau})K(\boldsymbol{\tau})d\boldsymbol{\tau} && \text{by Eqn. 4} && (7)
\end{aligned}$$

For a differentiable almost everywhere function $\mathcal{L}$, the weak gradient $g(\boldsymbol{\theta})$ is equal to $\nabla_{\boldsymbol{\theta}}\mathcal{L}$ almost everywhere. With a slight abuse of notation we can therefore write:

$$\nabla_{\boldsymbol{\theta}}\mathcal{L}_K(\boldsymbol{\theta}) = -\int_C \nabla_{\boldsymbol{\theta}}\mathcal{L}(\boldsymbol{\theta}-\boldsymbol{\tau})K(\boldsymbol{\tau})d\boldsymbol{\tau} \tag{8}$$

2.3 Gaussian Mollifiers

It is possible to use the standard Gaussian distribution $\mathcal{N}(0,\ \mathbf{I})$ as a mollifier $K(\cdot)$, as it satisfies the desired properties: it is infinitely differentiable, a sequence of properly rescaled Gaussian distributions converges to the Dirac delta function and it vanishes in infinity. With such a $K(\cdot)$ the gradient becomes:

$$\begin{aligned}
\nabla_{\boldsymbol{\theta}}\mathcal{L}_{K=\mathcal{N}}(\boldsymbol{\theta}) &= -\int_C \nabla_{\boldsymbol{\theta}}\mathcal{L}(\boldsymbol{\theta}-\boldsymbol{\tau})p(\boldsymbol{\tau})d\boldsymbol{\tau} && (9)\\
&= \mathrm{E}_{\boldsymbol{\tau}}[\ \nabla_{\boldsymbol{\theta}}\mathcal{L}(\boldsymbol{\theta}-\boldsymbol{\tau})\ ], \text{with } \boldsymbol{\tau} \sim \mathcal{N}(0,\ \mathbf{I}) && (10)
\end{aligned}$$

Exploiting the fact that a Gaussian distribution is a mollifier, we can focus on a sequence of mollifications indexed by scaling parameter ϵ introduced in Eqn. 2. A single element of this sequence takes the following form:

$$\begin{aligned}
\nabla_{\boldsymbol{\theta}}\mathcal{L}_{\mathcal{N},\epsilon}(\boldsymbol{\theta}) &= -\int_C \nabla_{\boldsymbol{\theta}}\mathcal{L}(\boldsymbol{\theta}-\boldsymbol{\tau})\epsilon^{-n}p(\boldsymbol{\tau}/\epsilon)d\boldsymbol{\tau} && (11)\\
&= \mathrm{E}_{\boldsymbol{\tau}}[\ \nabla_{\boldsymbol{\theta}}\mathcal{L}(\boldsymbol{\theta}-\boldsymbol{\tau})\ ], \text{with } \boldsymbol{\tau} \sim \mathcal{N}(0,\ \epsilon^2\mathbf{I}) && (12)
\end{aligned}$$

Replacing ϵ with σ yields a sequence of mollifications indexed by σ:

$$\nabla_{\boldsymbol{\theta}}\mathcal{L}_{\mathcal{N},\sigma}(\boldsymbol{\theta}) = \mathrm{E}_{\boldsymbol{\tau}}[\ \nabla_{\boldsymbol{\theta}}\mathcal{L}(\boldsymbol{\theta}-\boldsymbol{\tau})\ ], \text{with } \boldsymbol{\tau} \sim \mathcal{N}(0,\ \sigma^2\mathbf{I}) \tag{13}$$

with the following property (by Eqn. 2):

$$\lim_{\sigma\to 0} \nabla_{\boldsymbol{\theta}}\mathcal{L}_{\mathcal{N},\sigma}(\boldsymbol{\theta}) = \nabla_{\boldsymbol{\theta}}\mathcal{L}(\boldsymbol{\theta}) \tag{14}$$

An intuitive interpretation of the result is that σ determines the standard deviation of a mollifying Gaussian and is annealed in order to construct a sequence of gradually less "blurred" and closer approximations to $\mathcal{L}$. This is consistent with the property that when σ is annealed to zero we are optimizing the original function $\mathcal{L}$.

So far we obtained the mollified version $\mathcal{L}_K(\boldsymbol{\theta})$ of the cost function $\mathcal{L}(\boldsymbol{\theta})$ by convolving it with a mollifier $K(\boldsymbol{\theta})$. The kernel $K(\boldsymbol{\theta})$ corresponds to the average effect of injecting noise ξ sampled

[2] We omit for brevity the algebraic details involved with a translation of the argument.

from standard Normal distribution. The amount of noise controls the amount of smoothing. Gradually reducing the noise during training is related to a form of *simulated annealing* (Kirkpatrick et al., 1983). Similarly to the analysis in Mobahi (2016), we can write a Monte-Carlo estimate of $\mathcal{L}_K(\boldsymbol{\theta}) = (\mathcal{L} * K)(\boldsymbol{\theta}) \approx \frac{1}{N}\sum_{i=1}^{N} \mathcal{L}(\boldsymbol{\theta} - \xi^{(i)})$. We provide the derivation and the gradient of this equation in Appendix A.

The Monte-Carlo estimators of the mollifiers can be easily implemented with neural networks, where the layers typically have the form:

$$\mathbf{h}^l = \mathrm{f}(\mathbf{W}^l \mathbf{h}^{l-1}) \tag{15}$$

with $\mathbf{h}^{l-1}$ a vector of activations from the previous layer in the hierarchy, $\mathbf{W}^l$ a matrix representing a linear transformation and f an element-wise non-linearity of choice.

A mollification of such a layer can be formulated as:

$$\mathbf{h}^l = \mathrm{f}((\mathbf{W}^l - \xi^l)\mathbf{h}^{l-1}), \text{ where } \xi^l \sim \mathcal{N}(\mu, \sigma^2) \tag{16}$$

From Eqn. 16, it is easy to see that both weight noise methods proposed by Hinton & van Camp (1993) and Graves (2011) can be seen as a variation of Monte-Carlo estimate of mollifiers.

2.4 Generalized and Noisy Mollifiers

We introduce a generalization of the concept of mollifiers that encompasses the approach we explored here and that is targeted during optimization via a continuation method using stochastic gradient descent.

Definition 2.1. (Generalized Mollifier). A *generalized mollifier* is an operator, where $T_\sigma(f)$ defines a mapping between two functions, such that $T_\sigma : f \rightarrow f^*$.

$$\lim_{\sigma \to 0} T_\sigma f = f, \tag{17}$$

$$f^0 = \lim_{\sigma \to \infty} T_\sigma f \qquad \text{is an identity function} \tag{18}$$

$$\frac{\partial (T_\sigma f)(x)}{\partial x} \qquad \text{exists } \forall x, \sigma > 0 \tag{19}$$

In addition, we consider noisy mollifiers which can be defined as an expected value of a stochastic function $\phi(x, \xi)$ under some noise source ξ with variance σ:

$$(T_\sigma f)(x) = E_\xi[\phi(x, \xi_\sigma)] \tag{20}$$

Definition 2.2. (Noisy Mollifier). We call a stochastic function $\phi(x, \xi_\sigma)$ with input x and noise ξ a *noisy mollifier* if its expected value corresponds to the application of a generalized mollifier T_σ, as per Eqn. 20.

The composition of two noisy mollifiers sharing the same σ is also a noisy mollifier, since the three properties in the definition (Eqns. 17,18,19) are still satisfied. When $\sigma = 0$ no noise is injected and therefore the original function will be optimized. If $\sigma \rightarrow \infty$ instead, the function will become an identity function. Thus, for instance, if we mollify each layer of a feed-forward network except the output layer, when $\sigma \rightarrow \infty$ all the mollified layers will become identity function and the objective function of the network with respect to its inputs will be convex.

Consequently, corrupting separately the activation function of each level of a deep neural network (but with a shared noise level σ) and annealing σ yields a noisy mollifier for the objective function. This is related to the work of Mobahi (2016), who recently introduced a way of analytically smoothing of the non-linearities to help the training of recurrent networks. The differences of that approach from our algorithm is two-fold: we use a noisy mollifier (rather than an analytic smoothing of the network's non-linearities) and we introduce (in the next section) a particular form of the noisy mollifier that empirically proved to work well.

3 Method

We propose an algorithm to mollify the cost of a neural network which also addresses an important drawback of the previously proposed noisy training procedures: as the noise gets larger, it can

dominate the learning process and lead the algorithm to perform a random walk on the energy landscape of the objective function. Conversely in our algorithm, as the noise gets larger gradient descent minimizes a simpler (e.g. convex) but still meaningful objective function.

We define the desired behavior of the network in the limit cases where the noise is very large or very small, and modify the model architecture accordingly. Specifically, during training we minimize a sequence of increasingly complex noisy objectives $\mathrm{L} = (\mathcal{L}^1(\boldsymbol{\theta}; \xi_{\sigma_1}), \mathcal{L}^2(\boldsymbol{\theta}; \xi_{\sigma_2}), \cdots, \mathcal{L}^k(\boldsymbol{\theta}; \xi_{\sigma_k}))$ that we obtain by annealing the scale (variance) of the noise σ_i. Let us note that our algorithm satisfies the fundamental properties of the *generalized and noisy mollifiers* that we introduced earlier.

We use a noisy mollifier based on our definition in Section 2.4. Instead of convolving the objective function with a kernel:

1. We start the training by optimizing a convex objective function that is obtained by configuring all the layers between the input and the last cost layer to compute an identity function, i.e., by skipping both the affine transformations and the blocks followed by nonlinearities.
2. During training the level of noise p is annealed, allowing to gradually evolve from identity transformations to linear transformations between the layers.
3. Simultaneously, as we decrease the level of noise p allows the element-wise activation functions to gradually change from linear to be the nonlinear.

4 Simplifying the Objective Function for Feedforward Networks

For *every unit* of each layer, we either copy the activation (output) of the corresponding unit of the previous layer (the identity path in Figure 2) or output a noisy activation $\tilde{\mathbf{h}}^l$ of a non-linear transformation of it $\psi(\mathbf{h}^{l-1}, \boldsymbol{\xi}; \mathbf{W}^l)$, where $\boldsymbol{\xi}$ is noise, $\mathbf{W}^l$ is a weight matrix applied on $\mathbf{h}^{l-1}$ and $\boldsymbol{\pi}$ is a vector of binary decisions for each unit (the convolutional path in Figure 2):

$$\tilde{\mathbf{h}}^l = \psi(\mathbf{h}^{l-1}, \boldsymbol{\xi}; \mathbf{W}^l) \tag{21}$$

$$\phi(\mathbf{h}^{l-1}, \boldsymbol{\xi}, \boldsymbol{\pi}^l; \mathbf{W}^l) = \boldsymbol{\pi}^l \odot \mathbf{h}^{l-1} + (1 - \boldsymbol{\pi}^l) \odot \tilde{\mathbf{h}}^l \tag{22}$$

$$\mathbf{h}^l = \phi(\mathbf{h}^{l-1}, \boldsymbol{\xi}, \boldsymbol{\pi}^l; \mathbf{W}^l). \tag{23}$$

To decide which path to take, for each unit in the network, a binary stochastic decision is taken by drawing from a Binomial random variable with probability dependent on the decaying value of p^l:

$$\boldsymbol{\pi}^l \sim \mathrm{Bin}(p^l) \tag{24}$$

If the number of hidden units of layer $l-1$ and layer $l+1$ is not the same, we can either zero-pad layer $l-1$ before feeding it into the next layer or apply a linear projection to obtain the right dimensionality.

For $p^l = 1$, the layer computes the identity function leading to a **convex** objective. If $p^l = 0$ the layer computes the original non-linear transformation unfolding the full capacity of the model.

The pseudo-code for the mollified activations is reported in Algorithm 1.

Algorithm 1 Activation of a unit i at layer l.

$x_i \leftarrow \mathbf{w}_i^\top \mathbf{h}^{l-1} + b_i$ ▷ an affine transformation of $\mathbf{h}^{l-1}$
$\Delta_i \leftarrow \mathrm{u}(x_i) - \mathrm{f}(x_i)$ ▷ Δ_i is a measure of a saturation of a unit
$\sigma(x_i) \leftarrow (\mathrm{sigmoid}(a_i \Delta_i) - 0.5)^2$ ▷ std of the injected noise depends on Δ_i
$\xi_i \sim \mathcal{N}(0,\ 1)$ ▷ sampling the noise from a basic Normal distribution
$s_i \leftarrow\ p^l\ c\ \sigma(x_i) |\xi_i|$ ▷ Half-Normal noise controlled by $\sigma(x_i)$, const. c and prob-ty p^l
$\psi(x_i, \xi_i) \leftarrow \mathrm{sgn}(\mathrm{u}^*(x_i)) \mathrm{min}(|\mathrm{u}^*(x_i)|,\ |\mathrm{f}^*(x_i) + \mathrm{sgn}(\mathrm{u}^*(x_i))|s_i||) + \mathrm{u}(0)$ ▷ noisy activation
$\pi_i^l \sim \mathrm{Bin}(p^l)$ ▷ p^l controls the variance of the noise AND the prob of skipping a unit
$\tilde{h}_i^l = \psi(x_i, \xi_i)$ ▷ $\tilde{h}_i^l$ is a noisy activation candidate
$\phi(\mathbf{h}^{l-1}, \xi_i, \pi_i^l; \mathbf{w}_i) = \pi_i^l h_i^{l-1} + (1 - \pi_i^l) \tilde{h}_i^l$ ▷ make a HARD decision between h_i^{l-1} and $\tilde{h}_i^l$

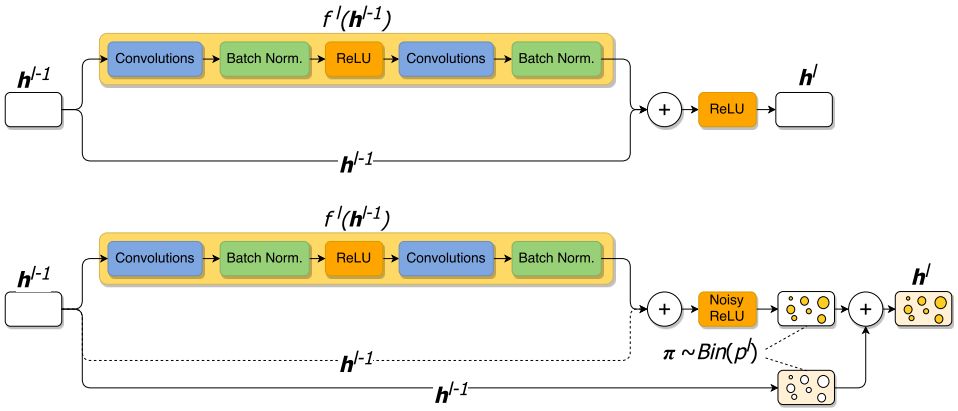

Figure 2: **Top:** Stochastic depth. **Bottom:** mollifying network. The dashed line represents the optional residual connection. In the top path, the input is processed with a convolutional block followed by a noisy activation function, while in the bottom path the original activation of the layer $l-1$ is propagated untouched. For each unit, one of the two paths in picked according to a binary stochastic decision $\boldsymbol{\pi}$.

5 Linearizing the network

In Section 2, we show that convolving the objective function with a particular kernel can be approximated by adding noise to the activation function. This method may suffer from excessive random exploration when the noise is very large.

We address this issue by bounding the element-wise activation function $\mathrm{f}(\cdot)$ with its linear approximation when the variance of the noise is very large, after centering it at the origin. The resulting function $\mathrm{f}^*(\cdot)$ is bounded and centered around the origin.

Note that centering the sigmoid or hard-sigmoid will make them symmetric with respect to the origin. With a proper choice of the standard deviation $\sigma(\mathbf{h})$, the noisy activation function becomes a linear function of the input when p is large, as illustrated by Figure 6.

Let $\mathrm{u}^*(x) = \mathrm{u}(x) - \mathrm{u}(0)$, where $\mathrm{u}(0)$ is the offset of the function from the origin, and x_i the i-th dimension of an affine transformation of the output of the previous layer $\mathbf{h}^{l-1}$: $x_i = \mathbf{w}_i^\top \mathbf{h}^{l-1} + b_i$. Then:

$$\psi(x_i, \xi_i; \mathbf{w}_i) = \mathrm{sgn}(\mathrm{u}^*(x_i))\min(|\mathrm{u}^*(x_i)|, |\mathrm{f}^*(x_i) + \mathrm{sgn}(\mathrm{u}^*(x_i))|s_i||) + \mathrm{u}(0) \tag{25}$$

The noise is sampled from a Normal distribution with mean 0 and whose standard deviation depends

a) b)

Figure 3: The figures show how to evolve the model to make it closer to a linear network. Arrows denote the direction of the noise pushing the activation function towards the linear function. **a)** The quasi-convex envelope established by a $|\mathrm{sigmoid}(\cdot)|$ around $|0.25x|$. **b)** A depiction of how the noise pushes the sigmoid to become a linear function.

on c:

$$s_i \sim \mathcal{N}(0,\ p\ c\ \sigma(x_i))$$

5.1 LINEARIZING RELU ACTIVATION FUNCTION

We have a simpler form of the equations to linearize ReLU activation function when $p^l \rightarrow \infty$. Instead of the complicated Eqn. 23. We can use a simpler equation as in Eqn. 26 to achieve the linearization of the activation function when we have a very large noise in the activation function:

$$s_i = \text{minimum}(|x_i|, p\sigma(x_i)|\xi|) \tag{26}$$

$$\psi(x_i, \xi_i, \mathbf{w}_i) = \text{f}(x_i) - s_i \tag{27}$$

6 MOLLIFYING LSTMS AND GRUS

In a similar vein it is possible to smooth the objective functions of LSTM and GRU networks by starting the optimization procedure with a simpler objective function such as optimizing a word2vec, BoW-LM or CRF objective function at the beginning of training and gradually increasing the difficulty of the optimization by increasing the capacity of the network.

For GRUs we set the update gate to $\frac{1}{t}$ – where t is the time-step index – and reset the gate to 1 if the noise is very large, using Algorithm 1. Similarly for LSTMs, we can set the output gate to 1 and input gate to $\frac{1}{t}$ and forget gate to $1 - \frac{1}{t}$ when the noise is very large. The output gate is 1 or close to 1 when the noise is very large. This way the LSTM will behave like a BOW model. In order to achieve this behavior, the activations $\psi(x_t, \xi_i)$ of the gates can be formulated as:

$$\psi(x_t^l, \xi) = \text{f}(x_t^l + p^l\sigma(x)|\xi|)$$

By using a particular formulation of $\sigma(x)$ that constraints it to be in expectation over ξ when $p^l = 1$, we can obtain a function for $\gamma \in \mathbb{R}$ within the range of $\text{f}(\cdot)$ that is discrete in expectation, but still per sample differentiable:

$$\sigma(x_t^l) = \frac{\text{f}^{-1}(\gamma) - x_t^l}{\text{E}_\xi[|\xi|]} \tag{28}$$

We provide the derivation of Eqn. 28 in Appendix B. The gradient of the Eqn. 28 will be a Monte-Carlo approximation to the gradient of $\text{f}(\mathbf{x}_t^l)$.

7 ANNEALING SCHEDULE FOR p

We used a different schedule for each layer of the network, such that the noise in the lower layers will anneal faster. This is similar to the linearly decaying probability of layers in Huang et al. (2016b). In our experiments, we use an annealing schedule similar to the inverse sigmoid rule in Bengio et al. (2015) with p_t^l,

$$p_t^l = 1 - \text{e}^{-\frac{k\mathbf{v}_t l}{tL}} \tag{29}$$

with hyper-parameter $k \geq 0$ at t^{th} update for the l^{th} layer, where L is the number of layers of the model. We stop annealing when the expected depth $p_t = \sum_{i=1}^{L} p_t^l$ reaches some threshold δ. $\mathbf{v}_t$ is a moving average of the loss[3] of the network, therefore the behavior of the loss/optimization can directly influence the annealing behavior of the network. Thus we will have:

$$\lim_{\mathbf{v}_t \to \infty} p_t^l = 1 \text{ and, } \lim_{\mathbf{v}_t \to 0} p_t^l = 0. \tag{30}$$

This has a desirable property: when the training-loss is high, the noise injected into the system will be large as well. As a result, the model is encouraged to do more exploration, while if the model converges the noise injected into the system by the mollification procedure will be zero.

[3]Depending on whether the model overfits or not, this can be a moving average of training or validation loss.

Figure 4: The learning curves of a 6-layers MLP with sigmoid activation function on 40 bit parity task.

	Test Accuracy
Stochastic Depth	93.25
Mollified Convnet	92.45
ResNet	91.78

Table 1: CIFAR10 deep convolutional neural network.

Furthermore, in our experiments we observe that training with noisy mollifiers can potentially be helpful for the generalization. This can be due to the noise induced to the backpropagation through the noisy mollification, that makes SGD more likely to converge to a flatter-minima (Hochreiter & Schmidhuber, 1997b) because the noise will help it escape from sharper local minima.

8 Experiments

In this section we mainly focus on training of difficult to optimize models, in particular deep MLPs with sigmoid or tanh activation functions. The details of the experimental procedure is provided in Appendix C.

8.1 Deep MLP Experiments

Deep Parity Experiments Training neural networks on a high-dimensional parity problem can be challenging (Graves, 2016; Kalchbrenner et al., 2015). We experiment on 40-dimensional parity problem with 6-layer MLP using sigmoid activation function. All the models are initialized with Glorot initialization Glorot et al. (2011) and trained with SGD with momentum. We compare an MLP with residual connections using batch normalization and a mollified network with sigmoid activation function. As can be seen in Figure 4, the mollified network converges faster.

Deep Pentomino Pentomino is a toy-image dataset where each image has 3 Pentomino blocks. The task is to predict whether if there is a different shape in the image or not (Gülçehre & Bengio, 2013). The best reported result on this task with MLPs is 68.15% accuracy (Gulcehre et al., 2014). The same model as ours trained without noisy activation function and vanilla residual connections scored 69.5% accuracy, while our mollified version scored 75.15% accuracy after 100 epochs of training on the $80k$ dataset.

CIFAR10 We experimented with deep convolutional neural networks of 110-layers with residual blocks and residual connections comparing our model against ResNet and Stochastic depth. We adapted the hyperparameters of the Stochastic depth network from Huang et al. (2016a) and we used the same hyperparameters for our algorithm. We report the training and validation curves of the three models in Figure 6 and the best test accuracy obtained early stopping on validation accuracy over 500 epochs in Table 1. Our model achieves better generalization than ResNet. Stochastic depth achieves better generalization, but it might be possible to combine both and obtain better results.

9 LSTM Experiments

Predicting the Character Embeddings from Characters Learning the mapping from sequences of characters to the word-embeddings is a difficult problem. Thus one needs to use a highly non-linear function. We trained a word2vec model on Wikipedia with embeddings of size 500 (Mikolov et al., 2014) with a vocabulary of size 374557.

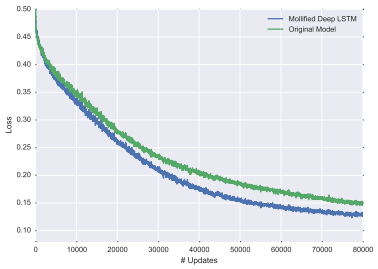

Figure 5: The training curve of a bidirectional-RNN that predicts the embedding corresponding to a sequence of characters.

	Test PPL
LSTM	119.4
Mollified LSTM	115.7

Table 2: 3-layered LSTM network on word-level language modeling for PTB.

LSTM Language Modeling We evaluate our model on LSTM language modeling. Our baseline model is a 3-layer stacked LSTM without any regularization. We observed that mollified model converges faster and achieves better results. We provide the results for PTB language modeling in Table 2.

10 Conclusion

We propose a novel method for training neural networks inspired by an idea of continuation, smoothing techniques and recent advances in non-convex optimization algorithms. The method makes learning easier by starting from a simpler model, solving a well-behaved problem, and gradually transitioning to a more complicated setting. We show improvements on very deep models, difficult to optimize tasks and compare with powerful techniques such as batch-normalization and residual connections. We also show that the mollification procedure improves the generalization performance of the model on two tasks.

Our future work includes testing this method on large-scale language tasks that require long training time, e.g., machine translation and language modeling.

Acknowledgements

We thank Nicholas Ballas and Misha Denil for the valuable discussions and their feedback. We would like to also thank the developers of Theano [4], for developing such a powerful tool for scientific computing Theano Development Team (2016). We acknowledge the support of the following organizations for research funding and computing support: NSERC, Samsung, Calcul Québec, Compute Canada, the Canada Research Chairs and CIFAR.

References

E. L. Allgower and K. Georg. *Numerical Continuation Methods. An Introduction*. Springer-Verlag, 1980.

Dzmitry Bahdanau, Kyunghyun Cho, and Yoshua Bengio. Neural machine translation by jointly learning to align and translate. *arXiv preprint arXiv:1409.0473*, 2014.

Samy Bengio, Oriol Vinyals, Navdeep Jaitly, and Noam Shazeer. Scheduled sampling for sequence prediction with recurrent neural networks. In *Advances in Neural Information Processing Systems*, pp. 1171–1179, 2015.

Yoshua Bengio, Jérôme Louradour, Ronan Collobert, and Jason Weston. Curriculum learning. In *Proceedings of the 26th annual international conference on machine learning*, pp. 41–48. ACM, 2009.

Léon Bottou. Online algorithms and stochastic approximations. In David Saad (ed.), *Online Learning in Neural Networks*. Cambridge University Press, Cambridge, UK, 1998.

[4] http://deeplearning.net/software/theano/

Kyunghyun Cho, Bart Van Merriënboer, Caglar Gulcehre, Dzmitry Bahdanau, Fethi Bougares, Holger Schwenk, and Yoshua Bengio. Learning phrase representations using rnn encoder-decoder for statistical machine translation. *arXiv preprint arXiv:1406.1078*, 2014.

Anna Choromanska, Mikael Henaff, Michael Mathieu, Gérard Ben Arous, and Yann LeCun. The loss surface of multilayer networks, 2014.

Yann Dauphin, Razvan Pascanu, Caglar Gulcehre, Kyunghyun Cho, Surya Ganguli, and Yoshua Bengio. Identifying and attacking the saddle point problem in high-dimensional non-convex optimization. In *NIPS'2014*, 2014.

Lawrence C Evans. Partial differential equations. *Graduate Studies in Mathematics*, 19:251–258, 1998.

Xavier Glorot, Antoine Bordes, and Yoshua Bengio. Deep sparse rectifier neural networks. In *AISTATS*, pp. 315–323, 2011.

Alex Graves. Practical variational inference for neural networks. In *Advances in Neural Information Processing Systems*, pp. 2348–2356, 2011.

Alex Graves. Adaptive computation time for recurrent neural networks. *arXiv preprint arXiv:1603.08983*, 2016.

Çağlar Gülçehre and Yoshua Bengio. Knowledge matters: Importance of prior information for optimization. *arXiv preprint arXiv:1301.4083*, 2013.

Caglar Gulcehre, Kyunghyun Cho, Razvan Pascanu, and Yoshua Bengio. Learned-norm pooling for deep feedforward and recurrent neural networks. In *Machine Learning and Knowledge Discovery in Databases*, pp. 530–546. Springer, 2014.

Caglar Gulcehre, Marcin Moczulski, Misha Denil, and Yoshua Bengio. Noisy activation functions. 2016.

Kaiming He, Xiangyu Zhang, Shaoqing Ren, and Jian Sun. Deep residual learning for image recognition. *arXiv preprint arXiv:1512.03385*, 2015.

Geoffrey Hinton, Li Deng, Dong Yu, George Dahl, Abdel rahman Mohamed, Navdeep Jaitly, Andrew Senior, Vincent Vanhoucke, Patrick Nguyen, Tara Sainath, and Brian Kingsbury. Deep neural networks for acoustic modeling in speech recognition. *Signal Processing Magazine*, 2012.

Geoffrey E Hinton and Drew van Camp. Keeping neural networks simple. In *ICANN'93*, pp. 11–18. Springer, 1993.

S. Hochreiter and J. Schmidhuber. Long short-term memory. *Neural Computation*, 9(8):1735–1780, 1997a.

Sepp Hochreiter and Jürgen Schmidhuber. Flat minima. *Neural Computation*, 9(1):1–42, 1997b.

Gao Huang, Yu Sun, Zhuang Liu, Daniel Sedra, and Kilian Weinberger. Deep networks with stochastic depth. *arXiv preprint arXiv:1603.09382*, 2016a.

Gao Huang, Yu Sun, Zhuang Liu, Daniel Sedra, and Kilian Q. Weinberger. Deep networks with stochastic depth. *CoRR*, abs/1603.09382, 2016b. URL `http://arxiv.org/abs/1603.09382`.

Sergey Ioffe and Christian Szegedy. Batch normalization: Accelerating deep network training by reducing internal covariate shift. *CoRR*, abs/1502.03167, 2015. URL `http://arxiv.org/abs/1502.03167`.

Nal Kalchbrenner, Ivo Danihelka, and Alex Graves. Grid long short-term memory. *arXiv preprint arXiv:1507.01526*, 2015.

S. Kirkpatrick, C. D. Gelatt Jr., , and M. P. Vecchi. Optimization by simulated annealing. 220: 671–680, 1983.

Y. LeCun, B. Boser, J. S. Denker, D. Henderson, R. E. Howard, W. Hubbard, and L. D. Jackel. Backpropagation applied to handwritten zip code recognition. *Neural Comput.*, 1 (4):541–551, December 1989. ISSN 0899-7667. doi: 10.1162/neco.1989.1.4.541. URL http://dx.doi.org/10.1162/neco.1989.1.4.541.

Tomas Mikolov, Kai Chen, Greg Corrado, and Jeffrey Dean. word2vec, 2014.

Volodymyr Mnih, Koray Kavukcuoglu, David Silver, Alex Graves, Ioannis Antonoglou, and Daan Wierstra. Playing atari with deep reinforcement learning. Technical report, arXiv:1312.5602, 2013.

Hossein Mobahi. Training recurrent neural networks by diffusion. *arXiv preprint arXiv:1601.04114*, 2016.

Arvind Neelakantan, Luke Vilnis, Quoc V. Le, Ilya Sutskever, Lukasz Kaiser, Karol Kurach, and James Martens. Adding gradient noise improves learning for very deep networks. *CoRR*, abs/1511.06807, 2015. URL http://arxiv.org/abs/1511.06807.

David Silver, Aja Huang, Chris J Maddison, Arthur Guez, Laurent Sifre, George Van Den Driessche, Julian Schrittwieser, Ioannis Antonoglou, Veda Panneershelvam, Marc Lanctot, et al. Mastering the game of go with deep neural networks and tree search. *Nature*, 529(7587):484–489, 2016.

Rupesh K Srivastava, Klaus Greff, and Jürgen Schmidhuber. Training very deep networks. In *Advances in Neural Information Processing Systems*, pp. 2368–2376, 2015.

Ilya Sutskever, Oriol Vinyals, and Quoc V Le. Sequence to sequence learning with neural networks. In *Advances in neural information processing systems*, pp. 3104–3112, 2014.

Christian Szegedy, Wei Liu, Yangqing Jia, Pierre Sermanet, Scott Reed, Dragomir Anguelov, Dumitru Erhan, Vincent Vanhoucke, and Andrew Rabinovich. Going deeper with convolutions. Technical report, Google, 2014.

Theano Development Team. Theano: A Python framework for fast computation of mathematical expressions. *arXiv e-prints*, abs/1605.02688, May 2016. URL http://arxiv.org/abs/1605.02688.

Francesco Visin, Kyle Kastner, Aaron Courville, Yoshua Bengio, Matteo Matteucci, and Kyunghyun Cho. Reseg: A recurrent neural network for object segmentation. *arXiv preprint arXiv:1511.07053*, 2015.

Wojciech Zaremba and Ilya Sutskever. Learning to execute. *arXiv preprint arXiv:1410.4615*, 2014.

Appendix

A Monte-Carlo Estimate of Mollification

$$\begin{aligned}\mathcal{L}_K(\boldsymbol{\theta}) \;&=\; (\mathcal{L} * K)(\boldsymbol{\theta}) \;=\; \int_C \mathcal{L}(\boldsymbol{\theta}-\xi)K(\xi)d\xi \text{ which can be estimated by a Monte Carlo:}\\ &\approx \frac{1}{N}\sum_{i=1}^{N}\mathcal{L}(\boldsymbol{\theta}-\xi^{(i)}),\ \text{where } \xi^{(i)} \text{ is a realization of the noise random variable } \xi\\ &\text{yielding } \frac{\partial \mathcal{L}_K(\boldsymbol{\theta})}{\partial \boldsymbol{\theta}}\\ &\approx \frac{1}{N}\sum_{i=1}^{N}\frac{\partial \mathcal{L}(\boldsymbol{\theta}-\xi^{(i)})}{\partial \boldsymbol{\theta}}.\end{aligned} \tag{31}$$

Therefore introducing additive noise to the input of $\mathcal{L}(\boldsymbol{\theta})$ is equivalent to mollification.

B DERIVATION OF THE NOISY ACTIVATIONS FOR THE GATING

Assume that $z_t^l = x_t^l + p_t^l \sigma(x)|\xi_t^l|$ and $\mathrm{E}_\xi[\psi(x_t^l, \xi)] = t$. Thus for all z_t^l,

$$\mathrm{E}_\xi[\psi(x_t^l, \xi_t^l)] = \mathrm{E}_\xi[\mathrm{f}(z_t^l)], \tag{32}$$

$$t = \mathrm{E}_\xi[\mathrm{f}(z_t^l)], \text{ assuming } \mathrm{f}(\cdot) \text{ behaves similar to a linear function:} \tag{33}$$

$$\mathrm{E}_\xi[\mathrm{f}(z_t^l)] \approx \mathrm{f}(\mathrm{E}_\xi[z_t^l]) \text{ since we use hard-sigmoid for } \mathrm{f}(\cdot) \text{ this will hold.} \tag{34}$$

$$\mathrm{f}^{-1}(t) \approx \mathrm{E}_\xi[z_t^l] \tag{35}$$

$$\tag{36}$$

As in Eqn. 32, we can write the expectation of this equation as:

$$\mathrm{f}^{-1}(t) \approx x_t^l + p_t^l \sigma(x) \mathrm{E}_\xi[\xi_t^l]$$

Corollary, the value that $\sigma(x_t^l)$ should take in expectation for $p_t^l = 1$ would be:

$$\sigma(x_t^l) \approx \frac{\mathrm{f}^{-1}(t) - x_t^l}{\mathrm{E}_\xi[\xi_t^l]}$$

In our experiments for $\mathrm{f}(\cdot)$ we used the hard-sigmoid activation function. We used the following piecewise activation function in order to use it as $\mathrm{f}^{-1}(x) = 4(x - 0.5)$. During inference we use the expected value of random variables π and ξ.

C EXPERIMENTAL DETAILS

C.1 MNIST

The weights of the models are initialized with Glorot & Bengio initialization Glorot et al. (2011). We use the learning rate of $4e-4$ along with RMSProp. We initialize a_i parameters of mollified activation function by sampling it from a uniform distribution, $\mathrm{U}[-2, 2]$. We used 100 hidden units at each layer with a minibatches of size 500.

C.2 PENTOMINO

We train a $6-$layer MLP with sigmoid activation function using SGD and momentum. We used 200 units per layer with sigmoid activation functions. We use a learning rate of $1e-3$.

C.3 CIFAR10

We use the same model with the same hyperparameters for both ResNet, mollified network and the stochastic depth. We borrowed the hyperparameters of the model from Huang et al. (2016a). Our mollified convnet model has residual connections coming from its layer below.

C.4 PARITY

The n-dimensional parity task is the task to figure out whether the sum of n-bits in a binary vector is even or odd. We use SGD with Nesterov momentum and initialize the weight matrices by using Glorot&Bengio initializationGlorot et al. (2011). For all models, we use the learning rate of $1e-3$ and momentum of 0.92. a_i is the parameters of mollified activation function are initialized by sampling from uniform distribution, $U[-2, 2]$.

C.5 LSTM LANGUAGE MODELING

We trained 2-layered LSTM language models on PTB word-level. We used the models with the same hyperparameters as in Zaremba & Sutskever (2014). We used the same hyperparameters for both the mollified LSTM language model and the LSTM. We use hard-sigmoid activation function for both the LSTM and mollified LSTM language model. We use hard-sigmoid activation function for the gates of the LSTM.

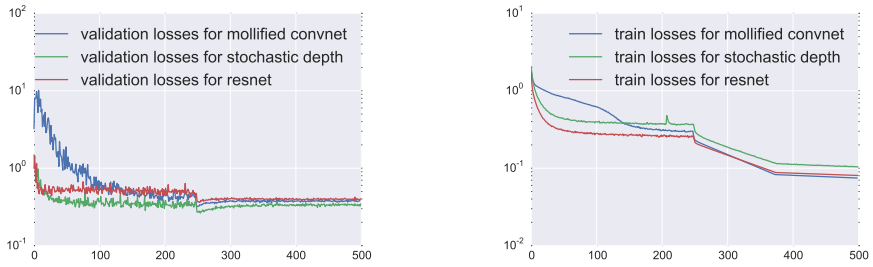

a) b)

Figure 6: Training and validation losses over 500 epochs of a mollified convolutional network composed by 110-layers. We compare against ResNet and Stochastic depth.

C.6 Predicting the Character Embeddings from Characters

We use $10k$ of these words as a validation and another $10k$ word embeddings as test set. We train a bidirectional-LSTM on top of each sequence of characters for each word and on top of the representation of bidirectional LSTM, we use a 5-layered $\tanh$-MLP to predict the word-embedding.

We train our models using RMSProp and momentum with learning rate of $6e-4$ and momentum 0.92. The size of the minibatches, we used is 64. As seen in Figure 5, mollified LSTM network converges faster.